A multi-Gaussian quadrature method of moments for simulating high Stokes number turbulent two-phase flows

Aymeric Vié, Christophe Chalons, Rodney Fox, Frédérique Laurent, Marc Massot

A multi-Gaussian quadrature method of moments for simulating high Stokes number turbulent two-phase flows

By A. Vié, C. Chalons, R. O. Fox, F. Laurent AND M. Massot

1. Motivation and objectives

With the great increase in computational resources, Large Eddy Simulation (LES) of industrial configurations is now an efficient and tractable tool. Numerous applications involve a liquid or solid disperse phase carried by a gaseous flow field (e.g., fuel injection in automotive or aeronautical engines, fluidized beds, and alumina particles in rocket boosters). To simulate this kind of flow, one may resort to a Number Density Function (NDF), which satisfies a kinetic equation. Solving for this NDF can make use of Lagrangian Monte-Carlo methods, but such approaches are expensive as the amount of numerical particles needed may be large. Moreover, such methods are not well adapted to high-performance computing because of the intrinsic inhomogeneity of the NDF in most of the applications of interest. To overcome these drawbacks, one can use Eulerian methods, which solve for the moments of the NDF using an Eulerian system of conservation laws.

In the context of Direct Numerical Simulation (DNS), Février *et al.* (2005) proposed the Mesoscopic Eulerian Formalism (MEF), which is a modeling framework to account for the effect of turbulence on a disperse phase. Basically, they introduced the statistical decomposition of the motion of particles into correlated and uncorrelated parts, the former of which is common between all particles at a specific location, the latter being induced by the history of each particle which crosses different vortices before reaching this specific location. Such a description is obtained by a statistical average over an ensemble of realization of the disperse phase conditioned by a realization of the gas phase. They also propose to model the effect of such a decomposition by solving for the Random Uncorrelated Energy (RUE), which is the energy of this uncorrelated motion. Closures for the stresses induced by the uncorrelated motion on the moments were initially proposed by Kaufmann *et al.* (2008), and recently Masi *et al.* (2011) have introduced new closures that rely on a priori study of the structure of these stresses. This model is able to simulate configurations up to large Stokes numbers related to the small eddies of turbulence (Kaufmann *et al.* 2008; Masi *et al.* 2011; Dombard 2011) but at moderate Stokes number based on the large coherent vortices of the flow. However, at high Stokes number, the statistical description of the trajectory crossings that enables the MEF will not be adapted, as the correlated part of the motion will also encounter deterministic trajectory crossings which may not change from one realization of the disperse phase to another.

To account for such Particle Trajectory Crossings (PTC) in the correlated motion of the spray, quadrature approaches can be used (Desjardin *et al.* 2008; Kah *et al.* 2010; Yuan & Fox 2011; Chalons *et al.* 2011). In such an approach, the velocity distribution is assumed to be a sum of Dirac δ-functions in velocity phase space. This way, we can have locally more than one velocity, which allows PTC. This type of method has proven

capable of describing trajectory crossings, for example in the academic case of Taylor-Green vortices (Kah *et al.* 2010; Yuan & Fox 2011). A drawback to this type of method is that it uses several moments. In 3D, 32 moments are needed, whereas 5 moments are used for the MEF only. But in fact quadrature approaches directly solve for the stresses that are modeled in the MEF. Choosing between MEF and quadrature approaches is then determined by the problem needed to be solved. For moderate Stokes flows, the MEF will be sufficient, but for high Stokes flows, quadrature approaches will be required in order to properly account for spray segregation and dynamics.

In the context of LES, the disperse phase will be influenced by the subgrid scales of the gas flow, leading to an additional velocity dispersion around the mean velocity of the particles. The LES extension of the MEF was already proposed in Moreau *et al.* (2010), and has even been applied in complex configurations (Riber *et al.* 2009; Martinez *et al.* 2009). For quadrature approaches, the first step of such an extension was proposed in Chalons *et al.* 2010, by means of a multi-Gaussian quadrature (MG). This method can account for PTC because of its multiple quadrature points in velocity phase space, and for subgrid scale effects by means of a Gaussian distribution around each quadrature point. Furthermore, the authors remark that such a system exhibits hyperbolic behavior in Riemann problems, i.e., there is no formation of δ-shocks due to PTC between more than two trajectories, which is not the case for Dirac δ-functions quadratures. Note that such a model can degenerate to a mono-Gaussian distribution for one quadrature point, and thus is expected to solve for a description of the disperse phase which may be equivalent to the MEF. Besides, it can also naturally degenerate to Dirac δ-functions quadratures in regions of very low subgrid scale agitation, a very nice property of this method.

Hence, this work aims to apply this method to a fully 2-D case, to demonstrate its efficiency in avoiding δ-shocks in a fully 2-D context, and to capture additional dynamics as compared to standard quadrature approaches. We begin by introducing the kinetic equation and its related moments problem. Then we will describe the 2-D multi-Gaussian quadrature which is used to close the moments problem, and the related algorithm used for moments evolution. Finally, the full method will be applied on 2-D Taylor-Green Vortices, and will be compared to CQMOM and Lagrangian results.

2. The moments problem

In this work, we aim at solving the NDF $f(t, \mathrm{x}, \mathrm{v})$ for $\mathrm{x} = (x, y)^t$ and $\mathrm{v} = (u, v)^t$ using the following 2-D kinetic equation:

$$\partial_t f + \mathrm{v} \cdot (\nabla_{\mathrm{x}} f) + \nabla_{\mathrm{v}} \cdot \mathrm{F} f = 0, \quad t > 0, \, \mathrm{x} \in \mathbb{R}^2, \, \mathrm{v} \in \mathbb{R}^2, \tag{2.1}$$

where $\nabla_{\mathrm{x}} = (\partial/\partial x, \partial/\partial y)^t$, $\nabla_{\mathrm{v}} = (\partial/\partial u, \partial/\partial v)^t$, $\mathrm{F} = (F_u, F_v)^t$ is the acceleration due to drag force. The exact solution to this problem is given by $f(t, \mathrm{x}, \mathrm{v}) = f(0, \mathrm{x} - \mathrm{v}t, \mathrm{v}) = f_0(\mathrm{x} - \mathrm{v}t, \mathrm{v})$. As we consider Stokes drag, the acceleration due to drag force is then

$$F_u = \frac{u_g - u}{\tau_p}, \qquad F_v = \frac{v_g - v}{\tau_p} \tag{2.2}$$

where $\mathrm{v}_g = (u_g, v_g)^t$ is the gas velocity. We thus define the bivariate moments

$$M_{i,j}(t, \mathrm{x}) = \int_{\mathrm{v}} u^i v^j f(t, \mathrm{x}, \mathrm{v}) \mathrm{d}\mathrm{v}, \quad i, j = 0, \ldots, N, \quad N \in \mathbb{N}.$$

The associated governing equations are easily obtained from (2.1):

$$\partial_t M_{i,j} + \partial_x M_{i+1,j} + \partial_y M_{i,j+1} = \frac{iM_{i-1,j}u_g + jM_{i,j-1}v_g - (i+j)M_{i,j}}{\tau_p}, \quad i,j \geq 0. \tag{2.3}$$

The main problem is that for a given set of moments, there are always some fluxes that are not defined, so that we need a closure for these fluxes. To solve this equation, we propose to use kinetic methods in order to ensure the realizability of the moment set. The main building block of this type of method is reconstruction of the NDF at the kinetic level starting from a finite moment set. The number of moments that we need is then imposed by the proposed reconstruction. Relying on this reconstruction in order to compute unknown fluxes, we thus define a kinetic finite volume scheme for convection. For the drag force source terms, all moments are already known in the simplified framework of the present study. Nevertheless, for the sake of generality in treating arbitrary drag force laws, we use a complementary quadrature dedicated to multi-Gaussian distributions.

3. 2-D kinetic model, multi-Gaussian quadrature

Here we propose to use a multi-Gaussian quadrature for reconstruction of the NDF. This choice stems from the need to be able to account for PTC, which is done by using multiple quadrature points, and from the fact that we aim at LES, so we account for a velocity dispersion around each quadrature point. Furthermore, we expect that the resulting system will be hyperbolic, unlike the Dirac δ-functions quadrature which is only weakly hyperbolic, and can generate δ-shock where PTC occur between more than two trajectories (Chalons *et al.* 2011). The simplest 2-D multi-Gaussian distribution function is defined by

$$f^{\mathrm{G}}(\mathrm{v}) = \sum_{\alpha=1}^{4} \frac{\rho_\alpha}{\sqrt{2\pi|\Sigma|}} \exp\left(-\frac{1}{2}(\mathrm{v}-\mathrm{v}_\alpha)^t \Sigma^{-1}(\mathrm{v}-\mathrm{v}_\alpha)\right), \quad \Sigma = \begin{bmatrix}\sigma_{11} & \sigma_{12}\\ \sigma_{12} & \sigma_{22}\end{bmatrix}, \tag{3.1}$$

where Σ is the covariance matrix. The same covariance matrix is used for all quadrature points†. In (3.1) there are 15 parameters: $(\rho_\alpha, u_\alpha, v_\alpha, \alpha = 1,\ldots,4)$ and $(\sigma_{11}, \sigma_{12}, \sigma_{22})$. So we need to solve for 15 moments which are chosen to be the 15 lowest order bi-variate moments:

$$\begin{bmatrix} M_{0,0} & M_{0,1} & M_{0,2} & M_{0,3} & M_{0,4} \\ M_{1,0} & M_{1,1} & M_{1,2} & M_{1,3} & \\ M_{2,0} & M_{2,1} & M_{2,2} & & \\ M_{3,0} & M_{3,1} & & & \\ M_{4,0} & & & & \end{bmatrix}. \tag{3.2}$$

These parameters must be found by solving a highly nonlinear system. To reduce the complexity of such a problem, we propose to use the main idea of the Conditional Quadrature Method of Moments (CQMOM) of Yuan & Fox (2011). In this approach, the authors aim at defining a quadrature approximation of the moment problem by means of a sum of Dirac δ-functions:

$$f_{cqmom} = \sum_{k=1}^{2}\sum_{l=1}^{2} \rho_k \rho_{k,l} \delta(u-u_k)\delta(v-v_{k,l}). \tag{3.3}$$

† This choice allows a simple and fully analytical inversion algorithm. Furthermore, this velocity dispersion is due to local subgrid mixing, which tends to homogeneity, so that equal Σ for each Gaussian can be an accurate approximation.

Using such a reconstruction is useful, because pure x moments depend only on ρ_k and u_k. Four parameters of the reconstruction are defined using a 1-D quadrature algorithm on pure x moments. Furthermore, using ρ_k and u_k, the authors demonstrate that it is possible to construct conditional moments for each u_k for which the 1-D quadrature algorithm can be applied to define $\rho_{k,l}$ and $v_{k,l}$ independently for each k. Using a conditional approach allows the full non-linear problem of dimension 12 to be reduced to three simpler problems of dimension 4, for which several studies propose accurate and efficient algorithms (Yuan & Fox 2011, Chalons *et al.* 2011). One problem in such a method is that we cannot control all the moment set, as we have only 10 parameters and 12 moments to control. The controlled moments are determined by the conditioning direction, and this choice depends on the physics we want to solve for. For convection, the conditioning direction is the transport direction. For other processes, the evolution of moments must be calculated for every permutation of conditioning direction; the total evolution is thus the mean of the evolution of each permutation, resulting in an algorithm which does not have a preferential direction.

Using this idea for the 2-D multi-Gaussian quadrature, the proposed reconstruction is then

$$f^{\mathrm{G}}(\mathrm{v}) = \sum_{\alpha=1}^{2}\sum_{\beta=1}^{2} \frac{\rho_\alpha \rho_{\alpha,\beta}}{\sqrt{2\pi|\Sigma|}} \exp\left(-\frac{1}{2}(\mathrm{v}-\mathrm{v}_{\alpha,\beta})^t \Sigma^{-1} (\mathrm{v}-\mathrm{v}_{\alpha,\beta})\right), \tag{3.4}$$

where $\mathrm{v}_{\alpha,\beta} = (u_\alpha, v_{\alpha,\beta})^t$. The full algorithm is then decomposed into two parts. In the following, we detail the 1-D algorithm for the first quadrature in the conditioning direction. Then we will give the structure of the iterative algorithm for the quadrature in the other direction.

Considering the five pure x moments $(M_{0,0}, M_{1,0}, M_{2,0}, M_{3,0}, M_{4,0})^t$, the 1-D algorithm proposed in Chalons *et al.* (2010) is used. For the NDF defined in Eq. 3.4, these moments are

$$\begin{cases} M^{\mathrm{G}}_{0,0} = \rho_1 + \rho_2, \\ M^{\mathrm{G}}_{1,0} = \rho_1 u_1 + \rho_2 u_2, \\ M^{\mathrm{G}}_{2,0} = \rho_1(\sigma_{11}^2 + u_1^2) + \rho_2(\sigma_{11}^2 + u_2^2), \\ M^{\mathrm{G}}_{3,0} = \rho_1 u_1(3\sigma_{11}^2 + u_1^2) + \rho_2 u_2(3\sigma_{11}^2 + u_2^2), \\ M^{\mathrm{G}}_{4,0} = \rho_1 u_1^2(6\sigma_{11}^2 + u_1^2) + \rho_2 u_2^2(6\sigma_{11}^2 + u_2^2) + 3\sigma_{11}^4(\rho_1 + \rho_2), \end{cases}$$

where the five unknowns ρ_1, ρ_2, u_1, u_2 and σ_{11}^2 are found by solving the nonlinear system $M_{i,0} = M^{\mathrm{G}}_{i,0},\ i = 0, \ldots, 4$. It is clearly equivalent to solving the system

$$\begin{cases} M_{0,0} = \rho_1 + \rho_2, \\ M_{1,0} = \rho_1 u_1 + \rho_2 u_2, \\ M_{2,0} - \sigma_{11}^2 M_0 = \rho_1 u_1^2 + \rho_2 u_2^2, \\ M_{3,0} - 3\sigma_{11}^2 M_1 = \rho_1 u_1^3 + \rho_2 u_2^3, \\ M_{4,0} - 6\sigma_{11}^2 M_2 + 3\sigma_{11}^4 M_0 = \rho_1 u_1^4 + \rho_2 u_2^4. \end{cases} \tag{3.5}$$

For $\mathbf{M} = (M_{0,0}, M_{1,0}, M_{2,0}, M_{3,0}, M_{4,0})^t$ such that $M_{0,0} > 0$, let us define

$$e_x = \frac{M_{0,0}M_{2,0} - M_{1,0}^2}{M_{0,0}^2}, \quad q_x = \frac{(M_{3,0}M_{0,0}^2 - M_{1,0}^3) - 3M_{1,0}(M_{0,0}M_{2,0} - M_{1,0}^2)}{M_{0,0}^3},$$

and

$$\eta_x = \frac{-3M_{1,0}^4 + M_{4,0}M_{0,0}^3 - 4M_{0,0}^2 M_{1,0}M_{3,0} + 6M_{0,0}M_{1,0}^2 M_{2,0}}{M_{0,0}^4}.$$

System (3.5) is well-defined on the phase space Ω given by Chalons *et al.* 2010:

$$\Omega = \{\, \mathbf{M} = (M_{0,0}, M_{1,0}, M_{2,0}, M_{3,0}, M_{4,0})^t,$$
$$M_{0,0} > 0, e_x > 0, \eta_x > e_x^2 + \frac{q_x^2}{e_x}, \text{ and } \eta_x \leq 3e_x^2 \text{ if } q_x = 0\}.$$

Moreover, σ^2 is given by the unique real root of the third-order polynomial

$$\begin{cases} \mathcal{P}(\sigma_0) = 2\sigma_0^3 + (\eta_x - 3e_x^2)\sigma_0 + q_x^2, \\ \sigma_0 = \sigma_{11}^2 - e_x. \end{cases}$$

The three roots of $\mathcal{P}(\sigma_0)$ can be found analytically (one is real, and two are complex conjugates). In the numerical algorithm for moment inversion, the three roots are found from the analytical expressions and the real root is determined by checking the magnitude of the imaginary parts. This method was found to be rapid and robust for all realizable values of e and q. When $M_0 > 0$, the 1-D moment-inversion algorithm then consists of the following three steps:

(*a*) Given moments $\mathbf{M}$ in Ω, compute e_x, q_x and η_x.
(*b*) Find real root of $\mathcal{P}(\sigma_0)$, and $\sigma_{11}^2 = e_x + \sigma_0$.
(*c*) Solve (3.5) according to Desjardin *et al.* (2008) to find ρ_1, ρ_2, u_1, u_2. In the case where $\sigma_{11}^2 = e_x$, we set $\rho_2 = u_2 = 0$ and $\rho_1 = M_{0,0}$, $u_1 = M_{1,0}/M_{0,0}$.When $M_{0,0} = 0$, we set $\rho_1 = \rho_2 = 0$, and without loss of generality, $\sigma_{11} = 0$ and $u_1 = u_2 = 0$. In the case $u_1 = u_2$, we set $\rho_1 = \rho_2$.

Now we need to determine the eight remaining parameters $\rho_{k,l}$, $v_{k,l}$, σ_{22} and σ_{12}. But contrary to the CQMOM, for now we are not able to use a simple method that will use the 1-D algorithm. So here we use a bounded secant iterative method:

(*a*) Given moments $(M_{0,0}, M_{0,1}, M_{0,2}, M_{0,3}, M_{0,4})^t$, compute e_v and q_v.
(*b*) Find real root of $\mathcal{P}(\sigma_0)$, and *initial guess* $\sigma_{22}^2 = e_v + \sigma_0$.
(*c*) Using $M_{2,2}$, σ_{11}, and σ_{22}, compute σ_{12}.
(*d*) Using CQMOM, construct a 2-D quadrature conditioned on u.
(*e*) Check whether $M_{0,4} = M_{0,4}^{\mathrm{G}}$. If not, update guess for σ_{22} and return to step (*c*) until convergence is achieved.

So far, such an algorithm has been shown to be reliable in most cases, but evaluation of σ_{12} has proved to be difficult in some cases. For the rest of the paper, we have chosen to set $\sigma_{12} = 0$, that is to include the whole of the covariance matrix (x, y) correlation into the choice of the abscissas, in order to avoid any difficulty in cases where several values can be obtained for σ_{12}, and we are not able to choose them based on a rigorous/physical argument. The results will prove to be accurate with this choice and we are in the process of developing a new approach for the quadrature which should improve this point dramatically (Chalons *et al.* 2012).

4. Moments evolution

In the following, we will describe how we are using the multi-Gaussian quadrature detailed in the previous section to build realizable and efficient numerical methods in order to account for drag force and convection. As we are using an operator splitting drag force and convection in each direction are treated separately.

4.1. *Drag force*

For pure drag, we want to solve the following equation:

$$\partial_t M_{i,j} = \frac{iM_{i-1,j}u_g + jM_{i,j-1}v_g - (i+j)M_{i,j}}{\tau_p}, \quad i,j \geq 0. \tag{4.1}$$

In this equation, all moments are known initially. An analytical derivation of the solution of Eq. (4.1) is possible in the case of Stokes drag, and assuming a constant gas velocity during the timestep. But to account for more complex physics (arbitrary drag laws, two-way coupling...), a supplementary quadrature step, dedicated for the multi-Gaussian distribution, is envisaged. Here, a 16-node quadrature is used†:

$$f(t,\mathrm{x},\mathrm{v}) = \sum_{\alpha=1}^{4}\sum_{\beta=1}^{4} \rho^*_{\alpha\beta}(t,\mathrm{x})\delta\left(u - u^*_\alpha(t,\mathrm{x})\right)\delta\left(v - v^*_{\alpha\beta}(t,\mathrm{x})\right), \tag{4.2}$$

defined using 48 moments found from the multi-Gaussian function in (3.1) [see Yuan & Fox (2011) for details]. This projection evolves with respect to 2×16 decoupled ordinary differential equations:

$$\frac{\mathrm{d}u^*_\alpha}{\mathrm{d}t} = -\frac{u^*_\alpha - u_g}{\tau_p}, \qquad \frac{\mathrm{d}v^*_{\alpha\beta}}{\mathrm{d}t} = -\frac{v^*_{\alpha\beta} - v_g}{\tau_p}, \tag{4.3}$$

where (u_g, v_g) is the gas velocity vector and τ_p the relaxation time scale that can account for Reynolds number effects. In the case of Stokes drag, this system is also analytically solved, considering that τ_p and u_g depend neither on velocity nor time‡:

$$u^*_\alpha(t+\Delta t,\mathrm{x}) = u^*_\alpha(t,x)\exp\left(-\frac{\Delta t}{\tau_p}\right) + u_g(t,\mathrm{x})\left(1-\exp\left(-\frac{\Delta t}{\tau_p}\right)\right), \tag{4.4}$$

$$v^*_{\alpha\beta}(t+\Delta t,\mathrm{x}) = v^*_{\alpha\beta}(t,x)\exp\left(-\frac{\Delta t}{\tau_p}\right) + v_g(t,\mathrm{x})\left(1-\exp\left(-\frac{\Delta t}{\tau_p}\right)\right). \tag{4.5}$$

Finally, the updated quadrature is used to reconstruct the updated moments:

$$M_{i,j}(t+\Delta t,\mathrm{x}) = \sum_{\alpha=1}^{4}\sum_{\beta=1}^{4} \rho^*_{\alpha\beta}(t,\mathrm{x})(u^*_{\alpha\beta}(t+\Delta t,\mathrm{x}))^i(v^*_{\alpha\beta}(t+\Delta t,\mathrm{x}))^j. \tag{4.6}$$

4.2. *Kinetic-based Flux-Splitting Scheme*

Here we propose a numerical scheme that makes use of the proposed reconstruction and an upwind resolution of the fluxes. As we use a dimensional splitting for convection, we derive the transport scheme for x direction only. The moment equations that we aim at solving are then

$$\begin{cases} \partial_t M_{0,0} + \partial_x M_{1,0} = 0, & \partial_t M_{0,2} + \partial_x M_{1,2} = 0, & \partial_t M_{4,0} + \partial_x \overline{M}_{5,0} = 0, \\ \partial_t M_{1,0} + \partial_x M_{2,0} = 0, & \partial_t M_{3,0} + \partial_x M_{4,0} = 0, & \partial_t M_{3,1} + \partial_x \overline{M}_{4,1} = 0, \\ \partial_t M_{0,1} + \partial_x M_{1,1} = 0, & \partial_t M_{2,1} + \partial_x M_{3,1} = 0, & \partial_t M_{2,2} + \partial_x \overline{M}_{3,2} = 0, \\ \partial_t M_{2,0} + \partial_x M_{3,0} = 0, & \partial_t M_{1,2} + \partial_x M_{2,2} = 0, & \partial_t M_{1,3} + \partial_x \overline{M}_{2,3} = 0, \\ \partial_t M_{1,1} + \partial_x M_{2,1} = 0. & \partial_t M_{0,3} + \partial_x M_{1,3} = 0, & \partial_t M_{0,4} + \partial_x \overline{M}_{1,4} = 0, \end{cases} \tag{4.7}$$

† As we expect that for one 2-D Gaussian distribution, 4 Dirac δ-functions are sufficient to capture the velocity dispersion, 16 nodes are used for 4 Gaussian distributions.

‡ Practically, it is possible to account for coupled drag force and evaporation by solving for an additional ODE for the droplet size, with the coupled system also having an analytical solution.

Overlined moments are those we need to reconstruct using the MG quadrature. To describe the complexity of the convective fluxes, a kinetic scheme is proposed. First we consider a finite-volume formulation (where c is the cell index):

$$\mathbf{M}_c^{n+1} = \mathbf{M}_c^n - \frac{\Delta t}{\Delta x}\left(\mathbf{F}_{c+1/2} - \mathbf{F}_{c-1/2}\right). \tag{4.8}$$

The fluxes are decomposed into positive and negative parts:

$$\mathbf{F}_{c+1/2} = \mathbf{F}^+_{c+1/2} + \mathbf{F}^-_{c+1/2}. \tag{4.9}$$

Positive and negative components are obtained by integrating the Gaussian quadrature on $\mathbb{R}^+$ or $\mathbb{R}^-$:

$$(F_{ij})^+_{c+1/2} = \int_v \int_0^\infty f(t, x_c, \mathrm{v}) u^{i+1} v^j du dv \tag{4.10}$$

$$(F_{ij})^-_{c+1/2} = \int_v \int_{-\infty}^0 f(t, x_{c+1}, \mathrm{v}) u^{i+1} v^j du dv. \tag{4.11}$$

This scheme is first order. In order to better resolve the fluxes in the framework of really multi-Gaussian distributions, a solution is proposed in Chalons *et al.* (2010). The idea is to apply an additional 16-node CQMOM quadrature on the moments set as done for drag force, by reconstructing 48 moments using the MG quadrature and the resulting set of high-order moments; from there, we can define a kinetic flux splitting finite volume scheme. Besides, the flux evaluation can be extended to quasi-second order by using the scheme developed in Vikas *et al.* (2011). The development of fully second order is an ongoing work of Kah *et al.* (2011), and will be of primary importance because the spatial segregation of particles is directly linked to the accuracy of the numerical scheme (Dombard 2011;Vié *et al.* 2011). As this work is devoted to a first qualitative analysis of the proposed strategy, we will use a first-order scheme.

5. Application to Taylor-Green vortices

Taylor-Green vortices consist of four counter-rotating vortices as in Figure 1:

$$U_g = \sin(2\pi x)\cos(2\pi y), \qquad V_g = -\cos(2\pi x)\sin(2\pi y). \tag{5.1}$$

This test case is expected to mimic the effect of turbulent structures on a disperse liquid phase. As in a turbulent flow, droplets are expected to accumulate in low vorticity zones, depending on their Stokes number. A critical Stokes number $\mathrm{St}_c = 1/8\pi$ is defined (de Chaisemartin 2009), and corresponds to the limit from which droplets can be ejected from their initial vortex. At time $t = 0$, droplets are distributed uniformly in the domain with zero velocity. The computational domain is composed of 200^2 cells.

In Figure 2, the MG quadrature and CQMOM are compared to the reference Lagrangian solution for $\mathrm{St} = 0.5\mathrm{St}_c$. Because the Stokes number is under its critical value, droplets are ejected from the centers of the vortices, but accumulate at the borders as they cannot cross the zero vorticity lines. This feature is captured by both Eulerian approaches, with some differences in the number density distribution along the center lines. In Figure 3, the number density is plotted against x (i.e. y) on the line $y = 0.5$ (i.e. $x = 0.5$). The CQMOM closure underestimates the droplet number density, whereas the MG closure reproduces more accurately the Lagrangian results. Furthermore, at the saddle points at each corner, a δ-shock is generated by the weakly hyperbolic system

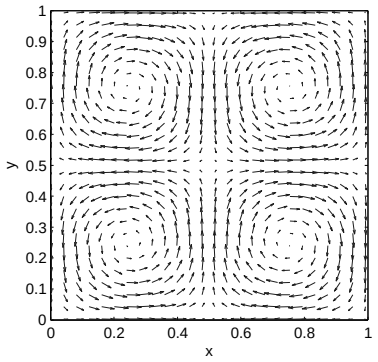

FIGURE 1. Taylor-Green vortices: gas velocity.

of the CQMOM closure, whereas the MG closure, which solves for a hyperbolic system, shows limited accumulations in relatively good agreement with the Lagrangian results.

In Figure 4, the results for $\mathrm{St} = 5\mathrm{St}_c$ are shown. Considering that the critical Stokes number is surpassed, trajectory crossing is observed. With the CQMOM and MG closures, we obtain qualitatively equivalent results, capturing the same structures, even if MG exhibits higher number density in the crossing zones. However, the two methods cannot capture the accumulation in the low vorticity zones. To further investigate the main difference between CQMOM and MG, the number density along lines $x = 1.0$ and $y = 1.0$ are plotted in Figure 5. First, as stated previously, the two methods do not reproduce the Lagrangian reference solution. But CQMOM also generates δ-shocks, unlike MG.

Finally, Figure 6 shows the results for $\mathrm{St} = 20\mathrm{St}_c$. Here the two Eulerian approaches cannot reproduce all of the fine structure in the Lagrangian solution. Furthermore, MG and CQMOM show different repartitions. To determine which is the more accurate, we investigate second-order moments $M_{1,1}$, $M_{2,0}$ and $M_{0,2}$ in Figures 7-9. First it is important to highlight that those moments are solved either by CQMOM or by MG. In approaches such as the MEF of Février *et al.* (2005), these moments are modeled using close-to-equilibrium assumptions. As the velocity distribution is really far from equilibrium in this configuration, such methods cannot capture the spatial dynamics. Here the moments results show that MG captures the structure of the velocity distribution more precisely than CQMOM. For example, the direction of the structures of moment M_{11} are oriented in the same direction as the Lagrangian results, which is not the case with CQMOM. Those difference lie in the ability of MG to account for multiple trajectory crossing by a pressure-like effect. This effect has the same limitation as the velocity dispersion in the MEF, i.e., it enables global effects of more than two trajectories crossings to be reproduced, but is not sufficient to reproduce exactly the full dynamics that we can see on the Lagrangian solution.

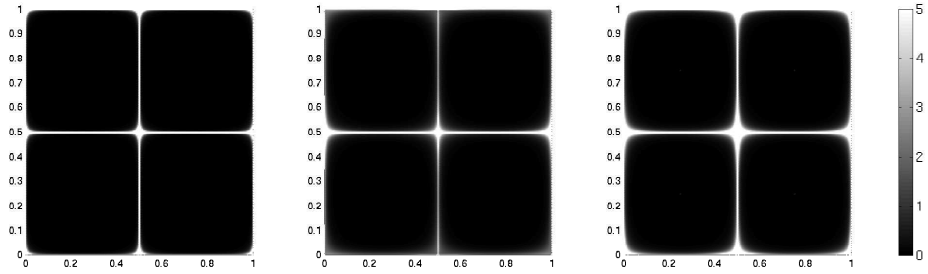

FIGURE 2. Taylor-Green vortices at $\mathrm{St} = 0.5\mathrm{St}_c$: droplet number density at time $t = 4$ for Lagrangian (left), CQMOM (center) and multi-Gaussian (right) simulations.

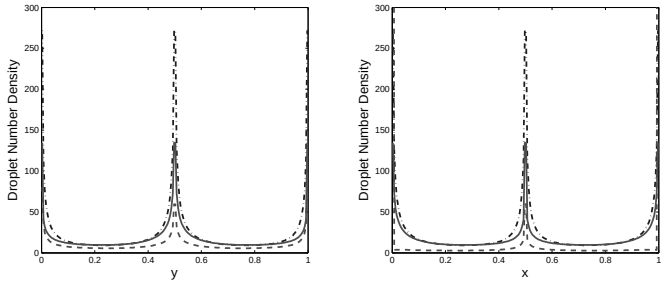

FIGURE 3. Taylor-Green vortices at $\mathrm{St} = 0.5\mathrm{St}_c$: droplet number density at time $t = 4$ on line $y = 0.5$ (left) and $x = 0.5$ (right) for Lagrangian (blue/dot-dashed), CQMOM (green/dashed) and multi-Gaussian (red/solid) simulations (scaled figures to focus on the central zone).

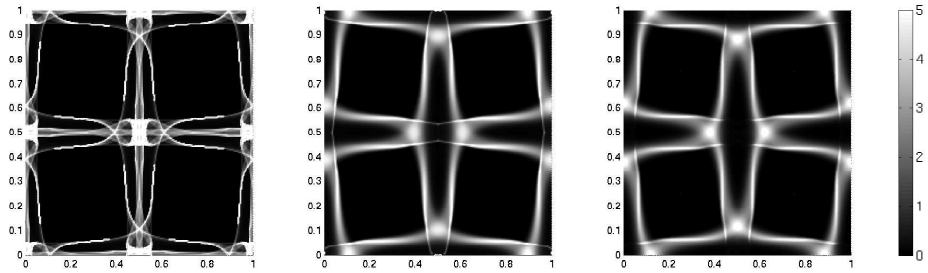

FIGURE 4. Taylor-Green vortices at $\mathrm{St} = 5\mathrm{St}_c$: droplet number density at time $t = 4$ for Lagrangian (left), CQMOM (center) and multi-Gaussian (right) simulations.

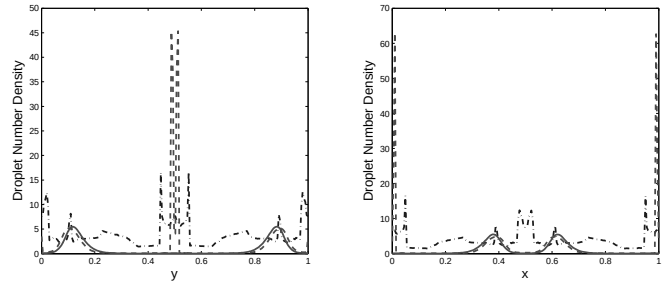

FIGURE 5. Taylor-Green vortices at $\mathrm{St} = 5\mathrm{St}_c$: droplet number density at time $t = 4$ on lines $y = 1$ (left) and $x = 1$ (right) for the Lagrangian (blue/dot-dashed), CQMOM (green/dashed) and multi-Gaussian (red/solid) simulations.

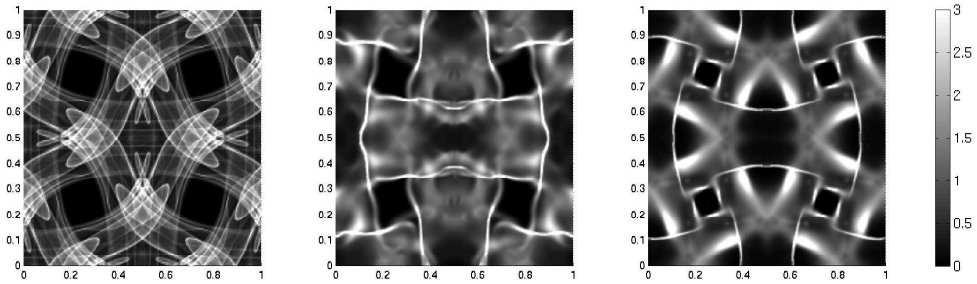

FIGURE 6. Taylor-Green vortices at $\mathrm{St} = 20\mathrm{St}_c$: droplet number density at time $t = 4$ for the Lagrangian (left), CQMOM (center) and multi-Gaussian (right) simulations.

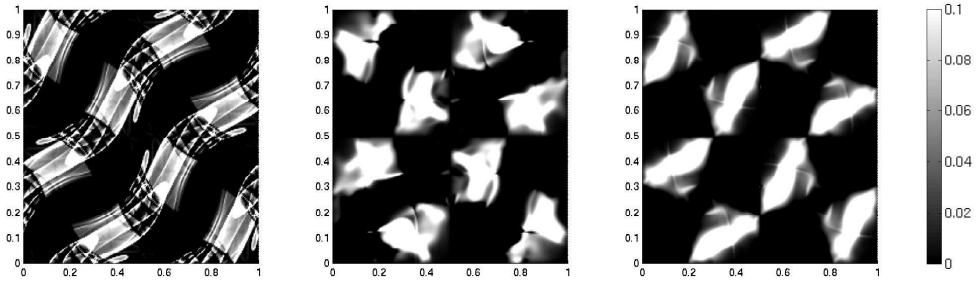

FIGURE 7. Taylor-Green vortices at $\mathrm{St} = 20\mathrm{St}_c$: $M_{1,1}$ at time $t = 4$ for the Lagrangian (left), CQMOM (center) and multi-Gaussian (right) simulations.

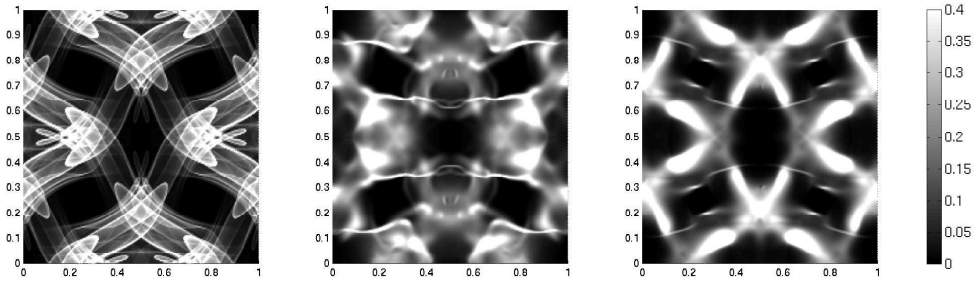

FIGURE 8. Taylor-Green vortices at $\mathrm{St} = 20\mathrm{St}_c$: $M_{2,0}$ at time $t = 4$ for the Lagrangian (left), CQMOM (center) and multi-Gaussian (right) simulations.

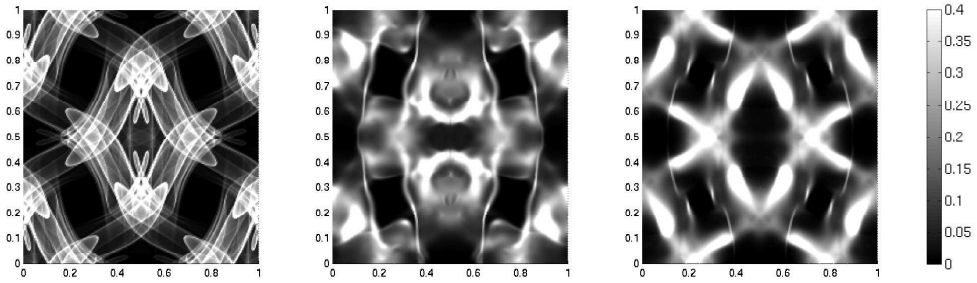

FIGURE 9. Taylor-Green vortices at $\mathrm{St} = 20\mathrm{St}_c$: $M_{0,2}$ at time $t = 4$ for the Lagrangian (left), CQMOM (center) and multi-Gaussian (right) simulations.

6. Conclusions and perspectives

This work has demonstrated the potential of the multi-Gaussian Quadrature Method of Moments. In the case of low or intermediate Stokes-number flows, the CQMOM and MG closures show similar results, but CQMOM exhibits δ-shocks when multiple trajectory crossings occur, whereas the potentially hyperbolic system of MG does not. For high Stokes flows, CQMOM cannot capture the dynamics while MG reproduces the global structure of the flow without generating any δ-shocks. The MG demonstrates its ability to solve and describe accurately the second-order moments (which are modeled in MEF approaches) and the importance of accounting for an additional velocity dispersion by mean of a Gaussian distribution to account for trajectory crossings between more than two trajectories, even in the case of DNS for which there is no subgrid scale for the gas phase that can generate a velocity dispersion.

For future perspectives, the 2-D MG inversion algorithm will be enhanced to avoid the iterative solution procedure in the secant method. A firmer mathematical study will also make use of the wave structure of the resulting system of PDEs (Chalons *et al.* 2012). A comprehensive comparison between MEF, CQMOM and MG approaches will be performed in order to characterize the main differences and similarities in terms of assumptions, modeling, and predictivity in DNS computations. Then, this formalism will be used in a LES context, by accounting for the effect of subgrid scales of the gas phase on the kinetic equation (Zaichik *et al.* 2009).

Acknowledgments

The authors wish to thank Parviz Moin and the Center for Turbulence Research at Stanford University for their hospitality and financial support during the CTR summer program of 2010. Support from the RTRA DIGITEO (Project MUSE, PI M. Massot) and Ecole Centrale Paris for the post-doctoral fellowship for A. Vié are gratefully acknowledged.

REFERENCES

de Chaisemartin, S. 2009 Eulerian models and numerical simulation of turbulent dispersion for polydisperse evaporation sprays. PhD thesis, Ecole Centrale Paris, France, available on TEL : http://tel.archives-ouvertes.fr/tel-00443982/en/.

Chalons, C., Fox, F. O., Laurent, F., Massot, M. & Vié, A. 2012 A multi-Gaussian quadrature-based moment method for dispersed multiphase flows. *SIAM Multiscale Modeling and Simulation* In preparation.

Chalons, C., Fox, R. O. & Massot, M. 2010 A multi-Gaussian quadrature method of moments for gas-particle flows in a LES framework. In *Proceedings of the Summer Program 2010, Center for Turbulence Research, Stanford University*, pp. 347–358. Stanford.

Chalons, C., Kah, D. & Massot, M. 2011 Beyond pressureless gas dynamics: quadrature-based velocity moment models. *Communication in Mathematical Sciences (Submitted for publication, in revision)* pp. 1–21, available online at http://hal.archives-ouvertes.fr/hal-00535782/en/.

Desjardin, O., Fox, R. & Villedieu, P. 2008 A quadrature-based moment method for dilute fluid-particle flows. *J. Comput. Phys.* **227**, 2514–2539.

Dombard, J. 2011 Direct numerical simulation of non-isothermal dilute sprays using the Mesoscopic Eulerian Formalism. PhD thesis, Université de Toulouse.

Février, P., Simonin, O. & Squires, K. D. 2005 Partitioning of particle velocities in gas-solid turbulent flow into a continuous field and a spatially uncorrelated random distribution: theoretical formalism and numerical study. *J. Fluid Mech.* **533**, 1–46.

Kah, D., Laurent, F., Fréret, L., de Chaisemartin, S., Fox, R., Reveillon, J. & Massot, M. 2010 Eulerian quadrature-based moment models for dilute polydisperse evaporating sprays. *Flow, Turbulence and Combustion* **85** (3–4), 649–676.

Kah, D., Vié, A., Chalons, C. & Massot, M. 2011 Second order scheme for quadrature-based velocity high order moment methods for disperse two-phase flows. *Annu. Res. Briefs, Center for Turbulence Research, Stanford University,* pp. 1–14.

Kaufmann, A., Moreau, M., Simonin, O. & Helie, J. 2008 Comparison between lagrangian and mesoscopic eulerian modelling approaches for inertial particles suspended in decaying isotropic turbulence. *J. Comput. Phys.* **227**, 6448–6472.

Martinez, L., Vie, A., Jay, S., Benkenida, A. & Cuenot, B. 2009 Large eddy simulation of fuel sprays using the eulerian mesoscopic approach. validations in realistic engine conditions. In *Proceedings of the 11th ICLASS, International Conference on Liquid Atomization and Spray Systems Vail, Colorado*, pp. 1–6.

Masi, E., Simonin, O. & Bédat, B. 2011 The mesoscopic eulerian approach for evaporating droplets interacting with turbulent flows. *Flow, Turbulence and Combustion* **86**, 563–583.

Moreau, M., Bédat, B. & Simonin, O. 2010 Development of gas-particle euler-euler LES approach: a priori analysis of particle sub-grid models in homogeneous isotropic turbulence. *Flow Turbulence and Combustion* **84** (2), 295–324.

Riber, E., Moureau, V., García, M., Poinsot, T. & Simonin, O. 2009 Evaluation of numerical strategies for large eddy simulation of particulate two-phase recirculating flows. *J. Comput. Phys.* **228**, 539–564.

Vié, A., Laurent, F. & Massot, M. 2011 A high order moment method for the simulation of polydisperse two-phase flows. In *Proceedings of the* 3^{rd} *INCA conference, Toulouse, France*.

Vikas, V., Wang, Z., Passalacqua, A. & Fox, R. O. 2011 Realizable high-order finite-volume schemes for quadrature-based moment methods. *J. Comput. Phys.* **230** (13), 5328 – 5352.

Yuan, C. & Fox, R. O. 2011 Conditional quadrature method of moments for kinetic equations. *J. Comput. Phys.* **230**, 8216 – 8246.

Zaichik, L., Alipchenkov, V. & Simonin, O. 2009 An eulerian approach for large eddy simulation of particle transport in turbulent flows. *J. Turbulence* **10** (9), 1–21.